



Contents lists available at ScienceDirect

## Resource-Efficient Technologies

journal homepage: [www.elsevier.com/locate/reffit](http://www.elsevier.com/locate/reffit)

# Synthesis of zinc oxide nanoparticles using plant leaf extract against urinary tract infection pathogen

J. Santhoshkumar, S. Venkat Kumar, S. Rajeshkumar\*

School of Biosciences and Technology, VIT University, Vellore 632014, TN, India

## ARTICLE INFO

### Article history:

Received 28 March 2017

Revised 5 May 2017

Accepted 12 May 2017

Available online xxx

### Keywords:

Green synthesis

Zinc oxide nanoparticles

Antimicrobial activity

Urinary tract infection pathogens

## ABSTRACT

In modern science, Nanotechnology is an ablaze field for the researchers. Zinc oxide nanoparticles (ZnO NPs) are known to be one of the most multifunctional inorganic nanoparticles with its application in treatment of urinary tract infection. Nanoparticles were synthesized using *Passiflora caerulea* fresh leaf extract and were characterized by UV-visible spectroscopy (UV-vis), X-ray diffractometer (XRD), Fourier transform infrared spectroscopy (FT-IR), Scanning electron microscopy (SEM), Energy dispersive analysis of x-ray (EDAX), Atomic force microscopy (AFM). Therefore, the study reveals an efficient, eco-friendly and simple method for the green synthesis of multifunctional ZnO NPs using *P. caerulea*. Urinary tract infection causing microbes were isolated from the disease affected patient urine sample. The synthesized nanoparticles have been tested against the pathogenic culture showed a very good zone of inhibition compared with plant extract. It indicates the biomedical capability of ZnO NPs.

© 2017 Tomsk Polytechnic University. Published by Elsevier B.V.

This is an open access article under the CC BY-NC-ND license.

(<http://creativecommons.org/licenses/by-nc-nd/4.0/>)

## 1. Introduction

Nanotechnology involves the use of materials having nanoscale dimensions in the range of 1–100 nm. Operating with nanomaterials has allowed researchers to have a much better understanding of biology. The green synthesis of nanoparticles has greatly reduced the use of physical and chemical methods. Various chemical methods have been proposed for the synthesis of zinc oxide nanoparticles (ZnO NPs), such as reaction of zinc with alcohol, vapor transport, hydrothermal synthesis, precipitation method etc [1–4]. The use of green synthesis method by the researchers is rapidly increasing due to usage of less toxic chemicals, eco-friendly nature and one step synthesis of nanoparticles [5]. The biological system involved in the green synthesis of nanoparticles are plants and their derivatives, microorganisms like bacteria, fungi, algae, yeast [6–9]. *P. caerulea* L. (Passifloraceae) is a medicinal plant native to South America, used against different pathogens causing various diseases such as diarrhea and their medicinal activity has been reported in many animal models [10]. Biosynthesis of ZnO NPs from plants such as *Aloe vera*, *Sargassum muticum*, *Eichhornia crassipes*, *Borassus flabellifer* fruit, and also in some bacterial and fungal species such as *Bacillus subtilis* and *Escherichia coli*, Ureolytic bac-

teria, *Lactobacillus plantarum* have been reported [11]. Nanoparticles synthesis within the size range of 10–100 nm have become an extensive research and concern due to their potential application in wide areas of science and technology. Metal oxide nanoparticles have been extensively used for medicinal purposes in the past decades. Metal oxide nanoparticles has environmental applications as it can act as catalyst which is helpful in reduction or elimination of the toxic hazardous chemicals from the environment [12]. Some of the metal oxide nanoparticles like, Fe<sub>3</sub>O<sub>4</sub>, TiO<sub>2</sub>, CuO and ZnO are thoroughly been investigated for their various biological activity [13]. Among those, ZnO NPs are used in the elimination of toxic chemicals like arsenic, sulfur from water sources owing to their large surface area by volume ratio than the bulk materials [14]. Zinc oxide has remarkable application in micro- electronics, diagnostics, optoelectronic devices, biomolecular detection, surface acoustic wave devices like laser devices, electromagnetic coupled sensor [1]. They can act as an alternative source for degradation of atmospheric pollutants [14,15].

They also have potential application in the field of medicine like drug delivery, biological activities such as antimicrobial, antioxidant, etc., and diagnosis of diseases. Antimicrobial activity of ZnO NPs against various pathogens such as *B. subtilis*, *Salmonella*, *Listeria monocytogenes*, *Staphylococcus aureus* and *E. coli* using disc diffusion method has been reported [16,17]. Also reported similar results by *Punica granatum* mediated synthesized ZnO NPs [19]. Some of the proposed mechanism responsible for antibacterial ac-

\* Corresponding author.

E-mail addresses: [ssrajeshkumar@hotmail.com](mailto:ssrajeshkumar@hotmail.com), [rajeshkumar.s@vit.ac.in](mailto:rajeshkumar.s@vit.ac.in) (S. Rajeshkumar).

<http://dx.doi.org/10.1016/j.reffit.2017.05.001>

2405-6537/© 2017 Tomsk Polytechnic University. Published by Elsevier B.V. This is an open access article under the CC BY-NC-ND license.

(<http://creativecommons.org/licenses/by-nc-nd/4.0/>)

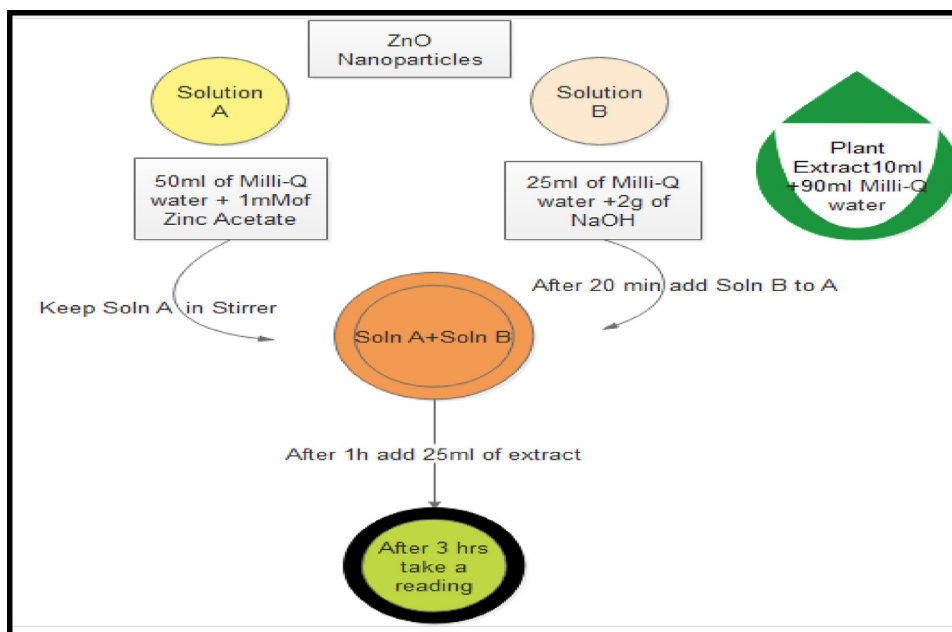


Fig. 1. Schematic representation of synthesis of ZnO NPs.

tivity of ZnO NPs includes disruption of the cell membrane, oxidative stress induction and generation of reactive oxygen species (ROS). It was reported that ZnO NP has showed high antibacterial activity against urinary infection disease [20]. Further the antibacterial activity of these biological synthesized ZnO NPs was evaluated against different pathogenic microorganisms. Our aim of the study is to synthesis ZnO NPs from the plant *P. caerulea* L. and their antibacterial activity against pathogens causing urinary tract infection.

## 2. Materials and methods

### 2.1. Plant collection

The leaves of *P. caerulea* L. (Passifloraceae) was collected in VIT. It is a medicinally important plant. Fresh green leaves, stem and flowers were harvested during the months of September to January.

### 2.2. Preparation of the plant extract

5 g of fresh leaves were washed with running tap water followed by Milli-Q water and then cut, and soaked in a 250 mL Erlenmeyer flask containing 100 mL Milli-Q. The solution was boiled at 70 °C for 8 min. The leaf extract was allowed to cool to room temperature, filtered through Whatman number-1 filter paper, and the filtrate was stored for further experimental use.

### 2.3. Synthesis of ZnO NPs

1 mM Zinc acetate [ $\text{Zn}(\text{O}_2\text{CCH}_3)_2(\text{H}_2\text{O})_2$ ] was dissolved in 50 ml Milli-Q water and kept in stirrer for 1 h respectively [4]. Then 20 mL of NaOH solution was slowly added into the Zinc acetate solution and 25 mL of plant extract was added to the same. (Fig. 1). The color of the reaction mixture was changed after 1 h of incubation time. The solution was left in stirrer for 3 h Yellow color appeared after the incubation time confirmed the synthesis of ZnO NPs. The precipitate was separated from the reaction solution by centrifugation at 8000 rpm at 60 °C for 15 min and pellet was col-

lected. Pellet was dried using a hot air oven operating at 80 °C for 2 h and preserved in air-tight bottles for further studies.

### 2.4. Characterization of biosynthesized ZnO NPs

Optical properties of ZnO NPs were characterized based on UV absorption spectra with the wavelength range of 300–500 nm. X-ray diffraction (XRD) analysis was performed on X-ray diffractometer (PAN analytical X-Pert PRO) operating at 30 kV and 40 mA. The pattern was recorded by  $\text{CuK}\alpha$  radiation with about 1.54060 Å X-ray crystallography is used for the determination of crystal density, purity and size of the nanoparticles. 2 mg of ZnO NPs was mixed with 200 mg of potassium bromide (FTIR grade) and pressed into a pellet for FTIR characterization. The sample pellet was placed into the sample holder and FTIR spectra were recorded in FTIR spectroscopy at a resolution of  $4\text{ cm}^{-1}$  [18]. Shape and size were analyzed by using SEM. Topography of the nanoparticles was characterized using Atomic Force Microscopy (AFM). Elemental compositions of the synthesized nanoparticle were characterized using Elemental Dispersion Analysis of X-ray (EDAX).

### 2.5. Antibacterial activity of synthesized ZnO NPs

The antibacterial activity of synthesized ZnO NPs was performed by agar disc diffusion method against urinary tract infection pathogens *Klebsiella pneumonia*, *B. subtilis*, *E. coli*, *Serratia sp.*, and *Streptococcus sp.* Fresh overnight culture of each strain was swabbed uniformly onto the individual plates. The 25  $\mu\text{l}$ , 50  $\mu\text{l}$  and 75  $\mu\text{l}$  of ZnO NPs solution impregnated disc were placed onto the plates and incubated for 24 h at 37 °C. Commercial antibiotic discs were placed as control. After incubation period got over, different levels of zonation formed around the disc was measured.

## 3. Results and discussion

### 3.1. Visual observation

ZnO NPs have attracted great attention because of their superior optical properties. Visual color change is the preliminary test for nanoparticle synthesis. (Fig. 2) represents the synthesis of ZnO

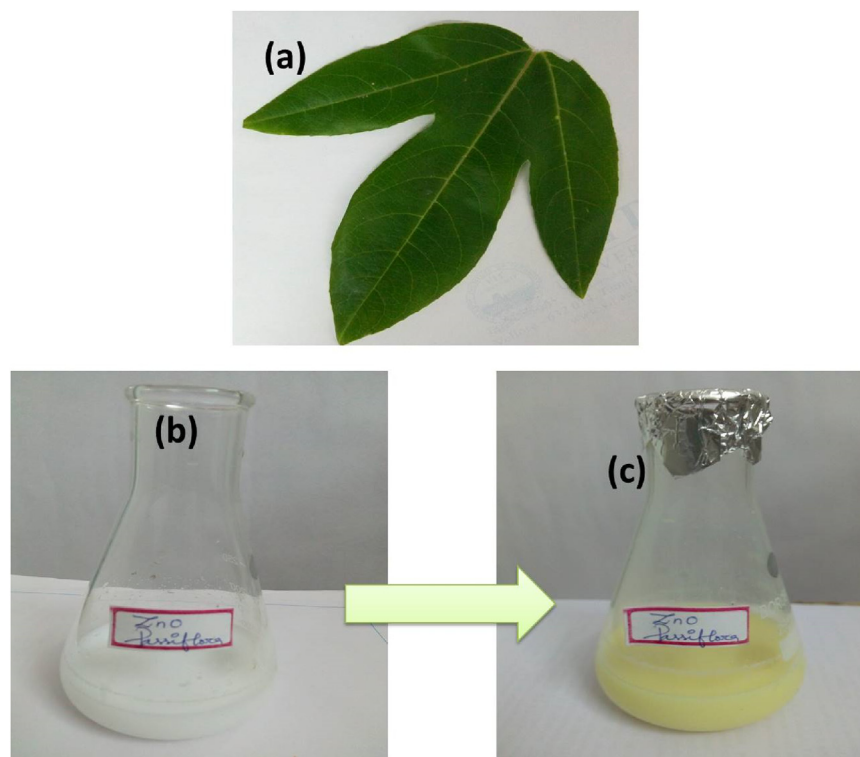


Fig. 2. Visual observation of ZnO NPs synthesis (a) *P. caerulea* leaves (b) initial color (c) final color change.

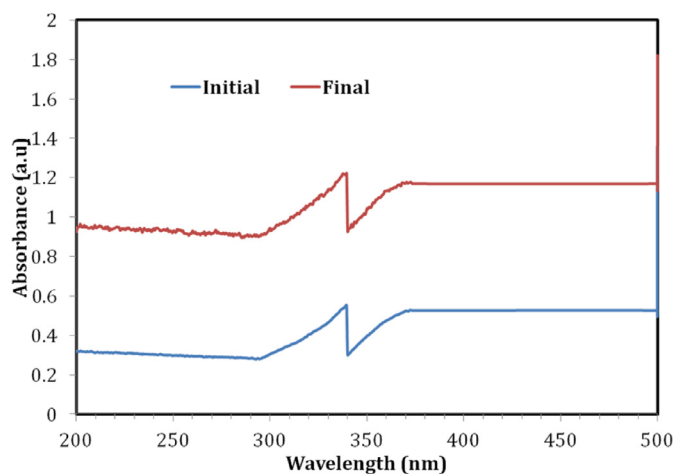


Fig. 3. UV-vis spectrum of ZnO NPs synthesized by *P. caerulea*.

NPs synthesized using freshly prepared *P. caerulea* fresh leaf extract. Color change from half white to pale yellow represents the synthesis of ZnO NPs.

### 3.2. UV-visible analysis

UV-visible spectroscopy is usually conducted to confirm the synthesis of ZnO NPs. Conducting electrons start oscillating at a certain wavelength range due to surface plasmon resonance (SPR) effect. (Fig. 3) represents the UV-visible spectra of freshly prepared ZnO NPs. Peak obtained at 380 nm clearly demonstrates the presence of ZnO NPs in the reaction mixture. Initial peak obtained at range of 420 nm got further raised due to oscillation of more electrons after 5 h which depicts the continuous synthesis of ZnO NPs.

### 3.3. SEM and EDAX

SEM analysis is done to visualize shape and size of nanoparticle. JSM6510LV Scanning electron microscope was used to determine the shape of *P. caerulea* capped ZnO NPs (Fig. 3). SEM images were seen in different magnification ranges like 2  $\mu\text{m}$ –200 nm which clearly demonstrated the presence of spherical shaped nanoparticle with mean average diameter of 70 nm [21]. (Fig. 4) shows the EDAX analysis, confirmed the presence of metallic zinc oxide in biosynthesized ZnO NPs. The composition obtained from EDAX analysis was Zinc (75.36%), Oxygen (22.36%), and Carbon (2.29%). The presence of carbon in trace amount indicates the involvement of plant phytochemical groups in reduction and capping of the synthesized ZnO NPs [22] (Fig. 5).

### 3.5. X-ray diffraction (XRD)

XRD Spectra provides an insight about the crystallinity of nanoparticle. (Fig. 6) represents XRD Spectra of ZnO NPs synthesized using *P. caerulea* fresh leaf extract. Size of the nanoparticle was calculated using Debye–Scherrer equation. X-ray diffraction peaks obtained at 31.8°, 34.44°, 36.29°, 47.57°, 56.61°, 67.96° and 69.07° corresponded to the lattice plane of (1 0 0), (0 0 2), (1 0 1), (1 0 2), (1 1 0), (1 1 2), (2 0 1) Suggesting the face-centered cubic (fcc) crystal structure of the nanoparticle. Joint Committee on Powder Diffraction Standards (JCPDS) was used as a reference to assign the lattice planes according to the peaks obtained. Average size of the synthesized nanoparticle was found to be. 37.67 nm.

$$D = \frac{K\lambda}{\beta \cos\theta}$$

where, D- particle size in nm,  $\lambda$ - X-ray wavelength,  $\beta$ - FWHM,  $\theta$ - Bragg's angle of reflection. Table 1 represents the FWHM value for every peak assigned for particle size calculation.

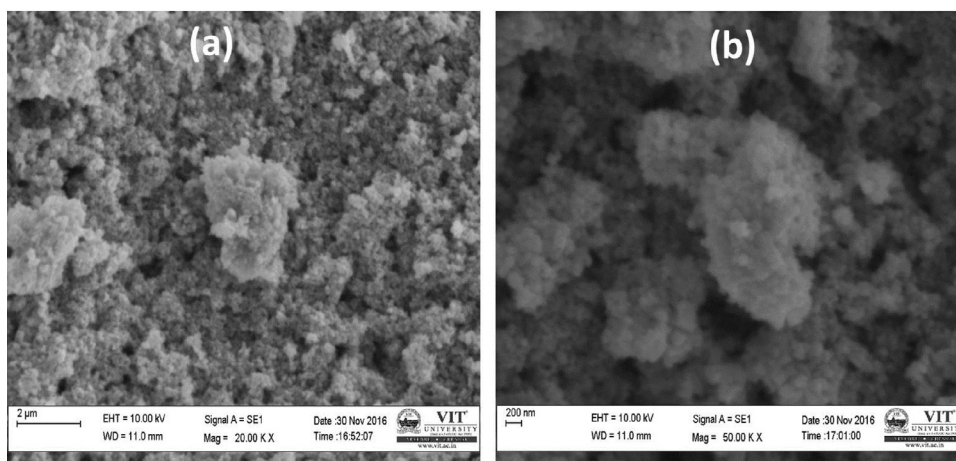


Fig. 4. SEM Images of ZnO NPs in different magnification ranges (a) 2  $\mu$ m (b) 200 nm.

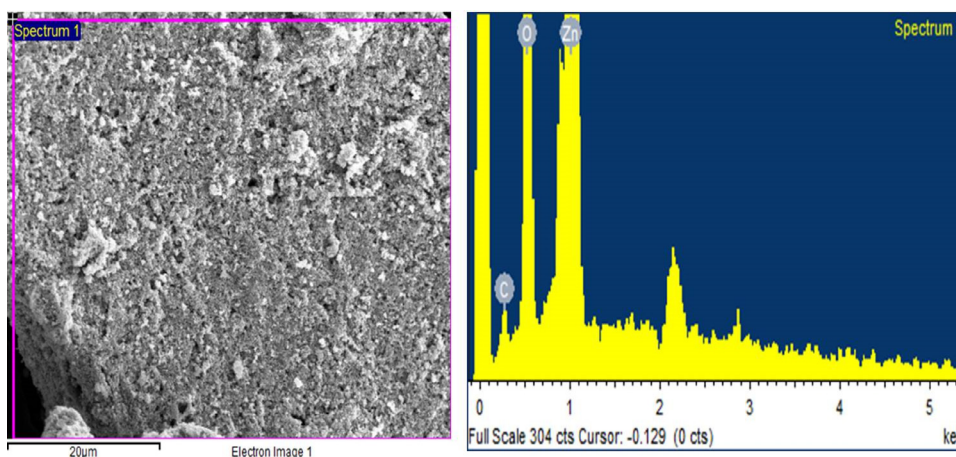


Fig. 5. EDAX Spectrum of ZnO NPs.

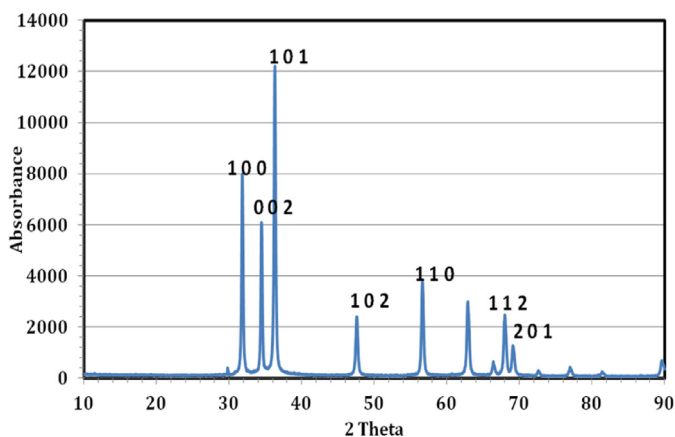


Fig. 6. XRD Spectrum of ZnO NPs.

### 3.6. FT-IR analysis

Substance-specific vibrations of the molecules lead to the specific signals obtained by IR spectroscopy. FT-IR spectra and functional group involved in ZnO NP synthesis illustrated peak in the range of 500–4000  $\text{cm}^{-1}$  (Fig. 7a and b and Table 2). Broad peak obtained at 3321.42 corresponded to OH stretching vibrations, peak in the range of 1541.12 and 1429.25 corresponded to C=C stretch

Table 1

Parameter calculation for average size calculation for nanoparticle.

$2\theta$	hkl	FWHM ( $\beta$ )	D (nm)
31.8	100	0.152	56.77
34.44	002	0.192	45.26
36.29	101	0.238	36.7
47.57	102	0.309	29.36
56.61	110	0.217	43.44
67.96	112	0.37	27.05
69.07	201	0.401	25.11

in aromatic ring and C=O stretch in polyphenols and C–N stretch of amide-I in protein. Weak peaks obtained at 1083.99, 1018.41 and 893.03 demonstrated the presence of C–O stretching in amino acid, C–N stretching and C–H bending respectively. A very ignorable peak obtained at 650.01 and 532.35 demonstrated the probable presence of C- Alkyl chloride and Hexagonal phase ZnO [23]. Plant extract itself had shown a broad range at 3304.06 corresponding to N–H stretch of amide group, sharp peaks obtained at 1635.64 and 1367.53 corresponded to C=C stretch alkane group and –C–H bending alkane group respectively. Weak peaks obtained at 1213.23 and 536.23 strongly depicted the presence of C–N stretch amine group and C–Br stretch alkyl Halide (Table 3).

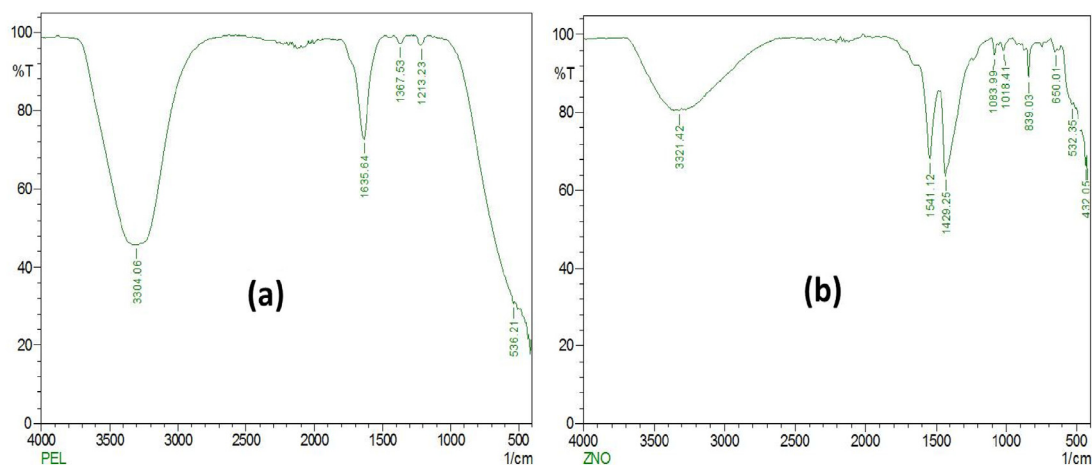


Fig. 7. FT-IR Spectrum of ZnO NPs (a) Plant extract (b) ZnO NPs with plant extract.

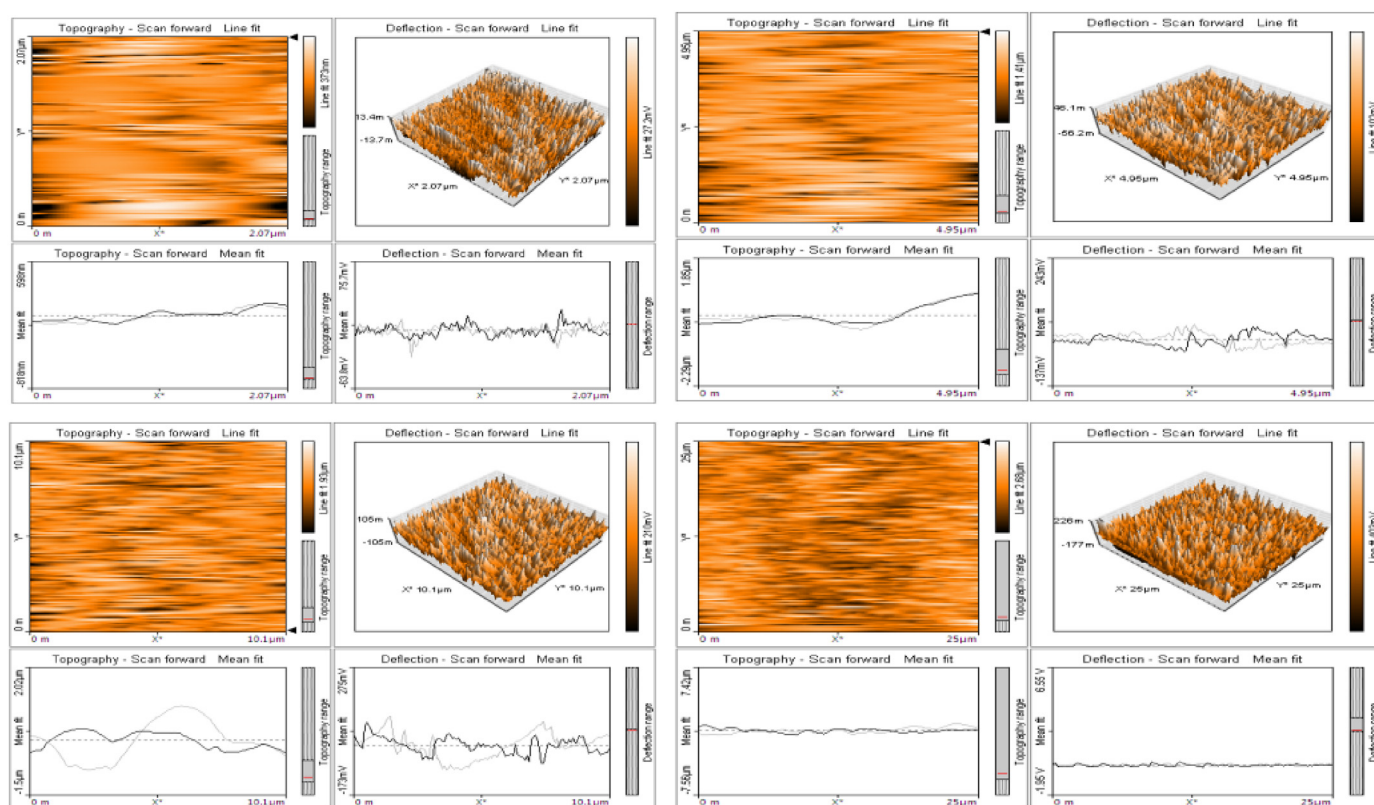


Fig. 8. AFM of ZnO NPs synthesized by plant extract.

### 3.7. AFM analysis

AFM analysis gives us insight about the topography, roughness of nanoparticles. AFM imaging was conducted in different magnification ranges of 1, 2, 5 and 25  $\mu\text{m}$ . AFM (Fig. 8) image clearly demonstrate smooth nanoparticle with capping of phytochemicals over the surface of nanoparticle [24].

### 3.8. Antimicrobial activity

Agar disc diffusion technique was adopted to perform the assay. Anti-bacterial effect of ZnO NPs was visualized against urinary tract infection pathogen like *E.coli*, *Streptococcus sp.*, *Enterococcus sp.*, *Klebsiella sp.* Ampicillin disc was used as a control. Results

clearly demonstrate that the nanoparticle showed anti-bacterial effect in a dose-dependent manner (Fig. 9 and Table 4). Maximum zone of inhibition was observed against a gram- bacterium (*E. coli*). Minimum zone of inhibition was observed against a gram+ bacteria (*Enterococcus sp.*). Different mechanism of action of nanoparticle against gram+ and gram- bacteria has been already reported in previous literature because of difference in structural composition. Zone of inhibition obtained using nanoparticle was much lower than the standard disc used which depicts the need of further engineering of nanoparticle to obtain desirable effects. The entire tests were done in triplicate. The zinc oxide nanoparticles are inhibit the microbial growth in *in-vitro* antimicrobial activities [18,19].

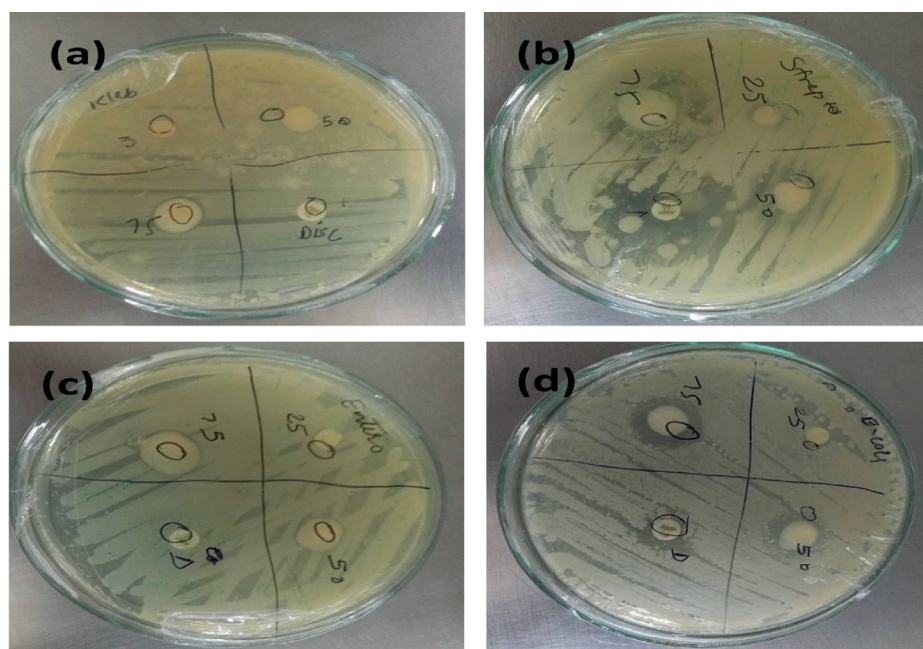


Fig. 9. Antibacterial activity of ZnO NPs against (a) *Klebsiella* sp. (b) *Streptococcus* sp. (c) *Enterococcus* sp. and (d) *E. coli*.

**Table 2**  
Functional involved in ZnO NPs synthesis analyzed by FT-IR.

S. No	Absorption peak (cm <sup>-1</sup> ) in ZnO NPs	Bond/functional groups
1.	3321.42	OH stretching vibrations
2.	1541.12	C=C stretch in aromatic ring and C=O stretch in polyphenols
3.	1429.25	C-N stretch of amide-I in protein
4.	1083.99	C-O stretching in amino acid
5.	1018.41	C-N stretching
6.	839.03	C-H bending
7.	650.01	C- Alkyl chloride
8.	532.35	Hexagonal phase ZnO

**Table 3**  
FT-IR Spectral peaks of plant extract.

S. No	Absorption peak (cm <sup>-1</sup> ) in ZnO NPs	Bond/functional groups
1.	3304.06	N-H stretch amide group
2.	1635.64	C=C stretch alkane group
3.	1367.53	C-H bending alkane group
4.	1213.23	C-N stretch amine group
5.	536.23	C-Br stretch alkyl Halide

**Table 4**  
Antibacterial activity of synthesized ZnO NPs against pathogenic bacteria.

Sample name	Zone of inhibition (mm)	Ampicillin		
		25 μl	50 μl	75 μl
<i>E. coli</i>	13	7.00 ± 0.58	10.33 ± 0.88	13.00 ± 1.16
<i>Enterococcus</i> sp.	19	7.33 ± 0.88	8.00 ± 1.00	9.33 ± 0.88
<i>Klebsiella</i> sp.	09	8.33 ± 0.88	9.33 ± 0.88	11.00 ± 1.16
<i>Streptococcus</i> sp.	04	8.33 ± 0.88	10.03 ± 1.16	11.67 ± 0.88

#### 4. Conclusion

Green synthesis of nanoparticles used in this experiment is found to be eco-friendly, non-toxic and less usage of chemicals compared to physical and chemical method. The presence of phytochemicals in the leaf extract itself helps in the synthesis of metal oxide nanoparticle by inducing oxidation and reduction reaction.

The functional groups of phytochemicals induce the nanoparticle synthesis were amines and alkanes that are widely seen in secondary metabolites such as terpenoids, flavonoids, alkaloids, etc. As a preliminary confirmation, the rapid synthesis of ZnO NP was measured using the UV-Visible spectroscopy at a maximum absorbance of 380 nm. Further the XRD analysis proved the crystalline nature of the ZnO NP, while the EDX analysis confirmed the presence of zinc and oxide ions in the nanoparticles. The SEM analysis of ZnO NP demonstrated the size approximately in the range of 30–50 nm. Also the anti-bacterial activity of ZnO NPs has proved that these can be used as potent anti-bacterial agent against urinary tract infection.

#### References

- [1] H. Mirzaei, M. Darroudi, Zinc oxide nanoparticles: biological synthesis and biomedical applications, *Ceram. Int.* 43 (2017) 907–914, doi:10.1016/j.ceramint.2016.10.051.
- [2] J. Pulit-Prociak, J. Chwastowski, A. Kucharski, M. Banach, Functionalization of textiles with silver and zinc oxide nanoparticles, *Appl. Surf. Sci.* 385 (2016) 543–553, doi:10.1016/j.apsusc.2016.05.167.
- [3] T.C. Taranath, B.N. Patil, Limonia acidissima L. leaf mediated synthesis of zinc oxide nanoparticles: a potent tool against Mycobacterium tuberculosis, *Int. J. Mycobacteriol.* 5 (2016) 197–204, doi:10.1016/j.ijmyco.2016.03.004.
- [4] P. Jamdagni, P. Khatri, J.S. Rana, Green synthesis of zinc oxide nanoparticles using flower extract of Nyctanthes arbor-tristis and their antifungal activity, *J. King Saud Univ.-Sci.* (2016), doi:10.1016/j.jksus.2016.10.002.
- [5] M. Sundrarajan, S. Ambika, K. Bharathi, Plant-extract mediated synthesis of ZnO nanoparticles using Pongamia pinnata and their activity against pathogenic bacteria, *Adv. Powder Technol.* 26 (2015) 1294–1299, doi:10.1016/j.apt.2015.07.001.
- [6] P. Rajiv, S. Rajeshwari, R. Venkatesh, Bio-Fabrication of zinc oxide nanoparticles using leaf extract of Parthenium hysterophorus L. and its size-dependent antifungal activity against plant fungal pathogens, *Spectrochimica Acta–Part A* 112 (2013) 384–387, doi:10.1016/j.saa.2013.04.072.
- [7] V. Anbukkarasi, R. Srinivasan, N. Elangovan, Antimicrobial activity of green synthesized zinc oxide nanoparticles from emblica officinalis, *Int. J. Pharm. Sci. Rev. Res.* 33 (2) (2015) 110–115.
- [8] G.R. Navale, D.J. Late, S.S. Shinde, JSM Nanotechnology & nanomedicine antimicrobial activity of ZnO nanoparticles against pathogenic bacteria and fungi, *JSM Nanotechnol. Nanomed.* 3 (2015).
- [9] S. Azizi, R. Mohamad, A. Bahadoran, S. Bayat, R.A. Rahim, A. Ariff, W.Z. Saad, Effect of annealing temperature on antimicrobial and structural properties of bio-synthesized zinc oxide nanoparticles using flower extract of Anchusa italica, *J. Photochem. Photobiol. B* 161 (2016) 441–449, doi:10.1016/j.jphotobiol.2016.06.007.

- [10] Chao Wang, Antibacterial effects of zinc oxide nanoparticles on *Escherichia coli* K88, *Afr. J. Biotechnol.* 11 (2012) 10248–10254, doi:[10.5897/AJB11.3703](https://doi.org/10.5897/AJB11.3703).
- [11] S. Vijayakumar, G. Vinoj, B. Malaikozhundan, S. Shanthi, B. Vaseeharan, Plec-tranthus amboinicus leaf extract mediated synthesis of zinc oxide nanoparticles and its control of methicillin resistant *Staphylococcus aureus* biofilm and blood sucking mosquito larvae, *Spectrochimica Acta-Part A* 137 (2015) 886–891, doi:[10.1016/j.saa.2014.08.064](https://doi.org/10.1016/j.saa.2014.08.064).
- [12] S. Gunalan, R. Sivaraj, V. Rajendran, Green synthesized ZnO nanoparticles against bacterial and fungal pathogens, *Prog. Nat. Sci.* 22 (2012) 693–700, doi:[10.1016/j.pnsc.2012.11.015](https://doi.org/10.1016/j.pnsc.2012.11.015).
- [13] S. Stankic, S. Suman, F. Haque, J. Vidic, Pure and multi metal oxide nanoparticles: synthesis, antibacterial and cytotoxic properties, *J. Nanobiotechnol.* 14 (2016) 73, doi:[10.1186/s12951-016-0225-6](https://doi.org/10.1186/s12951-016-0225-6).
- [14] S.T. Khan, J. Musarrat, A.A. Al-Khedhairi, Countering drug resistance, infectious diseases, and sepsis using metal and metal oxides nanoparticles: Current status, *Colloids Surf. B* 146 (2016) 70–83, doi:[10.1016/j.colsurfb.2016.05.046](https://doi.org/10.1016/j.colsurfb.2016.05.046).
- [15] F. Ghasemi, R. Jalal, Antimicrobial action of zinc oxide nanoparticles in combination with ciprofloxacin and ceftazidime against multidrug-resistant *Acinetobacter baumannii*, *J. Global Antimicrob. Resist.* 6 (2016) 118–122, doi:[10.1016/j.jgar.2016.04.007](https://doi.org/10.1016/j.jgar.2016.04.007).
- [16] J. Fowsiya, G. Madhumitha, N.A. Al-Dhabi, M.V. Arasu, Photocatalytic degradation of Congo red using *Carissa edulis* extract capped zinc oxide nanoparticles, *J. Photochem. Photobiol. B* 162 (2016) 395–401, doi:[10.1016/j.jphotobiol.2016.07.011](https://doi.org/10.1016/j.jphotobiol.2016.07.011).
- [17] R. Dobrucka, J. Długaszewska, Biosynthesis and antibacterial activity of ZnO nanoparticles using *Trifolium pratense* flower extract, *Saudi J. Biol. Sci.* 23 (2016) 517–523, doi:[10.1016/j.sjbs.2015.05.016](https://doi.org/10.1016/j.sjbs.2015.05.016).
- [18] V. Mishra, R. Sharma, Green synthesis of zinc oxide nanoparticles using fresh peels extract of *Punica granatum* and its antimicrobial activities, *Spectrochimica Acta-Part A* 143 (2015) 158–164, doi:[10.1016/j.saa.2015.02.011](https://doi.org/10.1016/j.saa.2015.02.011).
- [19] Y. Xie, Y. He, P.L. Irwin, T. Jin, X. Shi, Antibacterial activity and mechanism of action of zinc oxide nanoparticles against *Campylobacter jejuni*, *Appl. Environ. Microbiol.* 77 (2011) 2325–2331, doi:[10.1128/AEM.02149-10](https://doi.org/10.1128/AEM.02149-10).
- [20] G.D. Venkatasubbu, R. Baskar, T. Anusuya, C.A. Seshan, R. Chelliah, Toxicity mechanism of titanium dioxide and zinc oxide nanoparticles against food pathogens, *Colloids Surf. B* 148 (2016) 600–606, doi:[10.1016/j.colsurfb.2016.09.042](https://doi.org/10.1016/j.colsurfb.2016.09.042).
- [21] S. Raut, P.V. Thorat, R. Thakre, Green synthesis of zinc oxide (ZnO) nanoparticles using *Ocimum tenuiflorum* leaves, *Int. J. Sci. Res.* 14 (2013) 2319–2324 (IJSR) ISSN (Online Index Copernicus Value Impact Factor).
- [22] N. Bala, S. Saha, M. Chakraborty, M. Maiti, S. Das, R. Basu, P. Nandy, Green synthesis of zinc oxide nanoparticles using *Hibiscus subdariffa* leaf extract: effect of temperature on synthesis, anti-bacterial activity and anti-diabetic activity, *RSC Adv.* 5 (2015) 4993–5003, doi:[10.1039/C4RA12784F](https://doi.org/10.1039/C4RA12784F).
- [23] S. Yedurkar, C. Maurya, P. Mahanwar, Biosynthesis of zinc oxide nanoparticles using *Ixora coccinea* leaf extract—a green approach, *Open J. Synth. Theory Appl.* 5 (2016) 1–14, doi:[10.4236/ojsta.2016.51001](https://doi.org/10.4236/ojsta.2016.51001).
- [24] V. Femi, P.H. Prabha, P. Sudha, B. Devibala, A.L. Jerald, Anti bacterial effect of ZnO-Au nanocomposites, *Int. J. Biotechnol. Eng.* 1 (2011) 1–8.